Synergistic catalysis of carbon dioxide hydrogenation into methanol by yttria-doped ceria/γ-alumina-supported copper oxide catalysts: effect of support and dopant

Jenshi B. Wang [a], Hua-Kuo Lee [b], and Ta-Jen Huang [b,*]

[a] *Department of Chemical Engineering, I-Shou University, Kaohsiung, Taiwan, ROC*
[b] *Department of Chemical Engineering, National Tsing Hua University, Hsinchu, Taiwan, ROC*

Received 29 November 2001; accepted 31 May 2002

Methanol synthesis from carbon dioxide hydrogenation was studied over ceria/γ-alumina- and yttria-doped ceria (YDC)/γ-alumina-supported copper oxide catalysts to seek insight into the catalysis at metal–support interfaces. It was found that, in comparison with Cu/γ-Al_2O_3, the Cu/CeO_2/γ-Al_2O_3 and Cu/YDC/γ-Al_2O_3 catalysts exhibited substantial enhancement in activity and selectivity toward methanol formation. The extent of enhancement was augmented by increased ceria loading on γ-alumina and with increased yttria doping into ceria. The enhancement is inferred to result from the synergistic effect between copper oxide and surface oxygen vacancies of ceria.

KEY WORDS: carbon dioxide; hydrogenation; methanol; copper oxide; yttria-doped ceria; interfacial metal oxide–support interaction.

1. Introduction

Methanol synthesis from carbon dioxide hydrogenation has received considerable interest as one of the promising processes to exploit the carbon resources inherently contained in CO_2 into valuable chemicals and fuels. Copper-based catalysts such as Cu/ZnO in combination with Cr_2O_3 or Al_2O_3 are highly effective for this reaction [1–3]. While different studies have revealed a direct proportionality between methanol synthesis activity and total copper surface area [4–6], it has been shown that the activity of copper depends on the choice of support [6–8]. ZnO was perceived as playing the role of an enabling support, imparting a support effect of hydrogen spillover to promote a synergy between Cu and ZnO [6].

Among other metal/oxide combinations, Frost [9] demonstrated that activity enhancement of methanol formation could be obtained by using oxide promoted by metals other than copper, and attributed the support effect to the active centers formed between metal and surface oxygen vacancies of the support. The strong metal–support interaction appearing in ceria-supported palladium catalysts was reported to greatly improve the selectivity toward methanol synthesis from CO_2 hydrogenation [10,11]. X-ray diffraction analysis of the aforementioned catalysts reduced in hydrogen at 500 °C confirmed the formation of the Ce_2O_3 phase, suggesting the creation of new active centers at the metal–support interface. Although the importance of the support effect to upgrade catalysts has been recognized, there have been very few investigations on methanol synthesis from CO_2 hydrogenation over copper supported on oxygen-ion conducting oxides, particularly on the role of Ce^{3+} species in the reaction.

Since the concepts of strong metal–support interaction [12,13] and catalysis at the metal–support interface [14,15] were introduced, supports have been studied to explore advantages of the interaction. Oxygen-ion conducting oxides such as ceria, when heated to high temperature or treated under reducing atmospheres or doped with aliovalent cations [16,17], are known to impart metal–support interactions to enhance catalytic performances, due to their easy formation of oxygen vacancies [18,19] and excellent capabilities of oxygen storage/transport [20,21]. Thus, they have long been used in processes in automotive emission control [20,21], methanation and methanol synthesis [10,11,22–24].

Doped ceria has been a subject of considerable interest because the addition of dopants greatly increases the concentration of oxygen vacancies [16] or enhances catalytic activities for CO oxidation and NO reduction [25]. Yttria is one of the best possible dopants to modify the structural and chemical properties of ceria because the ionic radius and electronegativity of yttrium are close to those of cerium [26]. In practice, dispersing ceria or yttria-doped ceria (YDC) on γ-alumina support could be attractive, as this not only extends the interfacial boundary line between copper and ceria but also reduces the usage requirements of ceria or YDC [27,28].

* To whom correspondence should be addressed.
E-mail: tjhuang@che.nthu.edu.tw

1011-372X/02/1000-0079/0 © 2002 Plenum Publishing Corporation

The aim of this work is to elucidate the synergistic effect of Ce^{3+} in metal–support interaction on the activity enhancement of methanol formation catalyzed by copper oxide supported on ceria rather than to compare catalytic performances with that of Cu/ZnO. The effects brought about by doping ceria with yttria and the participation of the bulk Ce^{3+} oxygen vacancies in YDC on the observed catalytic properties are further examined in this study. For this purpose, Cu/γ-Al_2O_3, Cu/CeO_2/γ-Al_2O_3 and Cu/YDC/γ-Al_2O_3 catalysts with various yttria contents in ceria and two different ceria or YDC loading levels on γ-alumina were prepared and characterized by X-ray diffraction and temperature-programmed reduction (TPR). Activity tests were carried out to evaluate the performance of these catalysts with regard to the synergistic effect of Ce^{3+} in metal–support interaction.

2. Experimental

2.1. Support, catalyst preparation, and characterization

The YDC/γ-alumina supports were prepared by a co-impregnation method. Appropriate amounts of $Ce(NO_3)_3{\cdot}6H_2O$ (99.9%, Strem) and $Y(NO_3)_3{\cdot}6H_2O$ (99.9%, Strem) were dissolved in deionized water, followed by the addition of γ-alumina (99.9%, 2–3 μm, High Purity Chemicals Institute, Japan). The slurry was then stirred for 7 h. After evaporating excess water at *ca.* 60 °C, the slurry was dried in air at 120 °C for 12 h, calcined in air at 300 °C for 2 h and at 700 °C for 4 h, and then immediately quenched in water to maintain a cubic fluorite-type structure of the YDC support. The yttria content in the γ-alumina-supported YDC is 0, 5, 10, 15 or 20 mol%.

The copper catalysts were prepared by impregnating supports with an appropriate amount of aqueous solution of $Cu(NO_3)_2{\cdot}3H_2O$ (99.999%, Strem) for 6 h. After evaporating excess water at 80 °C, the catalysts were dried in air at 120 °C for 12 h, and then calcined in air at 260 °C for 1.5 h and at 500 °C for 3.5 h. The calcination of the supports and catalysts was conducted by passing air at the rate of 1 l/min, and by raising temperature at the rate of 10 °C/min from room temperature.

The BET surface areas of the catalysts were determined by means of nitrogen physisorption, applying a thermal conductivity detector instrument (Quantachrome). X-ray diffraction (XRD) patterns of the samples were recorded with a scanning speed of 1°/min on a Scintag XRD-2000 diffractometer using Cu K_{α_1} radiation. Samples for XRD were removed from the reactor after TPR under an inert atmosphere at room temperature and then were analyzed by XRD immediately.

2.1.1. Definition of catalyst symbols

1. The number in front of Cu is the copper loading in wt%, which is calculated with respect to the weight of YDC/γ-Al_2O_3 composite support, while 5CuAl stands for the catalyst 5Cu/γ-Al_2O_3.
2. The number x in YxCe is the yttria content in mol%, which is evaluated based on the yttria plus ceria moles of YDC supported on γ-alumina.
3. The number following Ce or YxCe is the CeO_2 or YDC loading in wt%, which is calculated only with respect to the weight of γ-alumina.

2.2. Temperature-programmed reduction

Temperature-programmed reduction (TPR) was carried out by using 10% hydrogen in nitrogen as a reducing gas in a conventional TPR reactor. The reactor was made up of an 8-mm i.d. quartz U-tube with catalyst samples of 200 mg mounted on loosely packed quartz wool. The outlet of the reactor was connected to a glass column packed with molecular sieve 5 Å in order to remove the moisture produced from reduction. The flow rate of the reducing gas was kept at 30 ml/min by a mass flow controller. The temperature of the reactor was raised from room temperature to 800 °C at the rate of 10 °C/min by a temperature programmable controller (Eurotherm, Model 815P). The rate of hydrogen consumption was measured by a thermal conductivity detector and recorded by an on-line personal computer. The peak areas of TPR were separated and integrated by this computer using special software.

2.3. Activity measurement

The pre-reduction and activity tests of the catalysts were conducted in a continuous flow reactor charged with 1.0 g of catalyst sample. The reactor was of a 33.4-mm i.d. stainless steel tube imbedded in an insulated electric furnace (Mitsubishi Electric), equipped with a Eurotherm-815P temperature controller, to achieve an isothermal environment. Silica sand of 10–20 mesh was utilized to fix the catalyst bed in which a K-type thermocouple was inserted to measure and control bed temperature.

The procedure of pre-reduction included heating the catalysts in flowing hydrogen (99.9995%, Sanfu, Taiwan) at 100 ml/min for 8 h at 250 °C under a pressure of 10 kg/cm^2. After termination of the reduction, a gaseous mixture of carbon dioxide (99.99%, Sanfu) and hydrogen with a composition of $H_2:CO_2 = 5:1$, as regulated by Hastings HFC-202 mass flow controllers, was fed to the catalyst bed at a total flow rate of 100 ml/min. At the chosen gas flow rate, reactant feed composition, and amount of catalyst used in the activity tests, the conversions of CO_2 are typically less than 18%. Before entering the reactor, the hydrogen gas was purified by passing through a purification system (Analysis Automation Ltd., Model 1929), and carbon dioxide through a filter to eliminate trace amounts of impurities. The reaction was carried out isothermally at 250 °C under 30 kg/cm^2. The activity measurement was made when a

steady state had been reached. The reactor outflow was analyzed on-line by two gas chromatographs (Shimadzu, GC-8A) in series equipped with thermal conductivity detectors. The first GC with a Porapak Q column was for analyzing CH_3OH and H_2O, while the second one with a silica gel column was primarily for the analyses of H_2, CO, CH_4 and CO_2. A cold trap was installed after the first GC to condense CH_3OH and water produced in the reaction.

3. Results and discussion

3.1. Surface area and XRD characterization

As shown in figure 1, the BET areas of the various supports and catalysts decrease due to ceria and copper oxide loading and also with increasing yttria doping into ceria. The decrease in BET areas of the supports and catalysts after calcinations is presumably ascribed to the plugging of some micropores by copper oxide and by the loading of ceria because of the non-porous nature of copper oxide and ceria-containing materials [21,28,29].

Figure 2 displays the XRD patterns of the co-impregnated YxCe20 supports and the bulk Y5Ce100 support made by the co-precipitation method, all under the same calcination conditions. Irrespective of yttria contents, the diffraction lines characteristic of yttria are not discernible from the XRD patterns of these supports, which exhibit only the peaks characteristic of ceria. X-ray diffraction analyses of the modified ceria confirmed

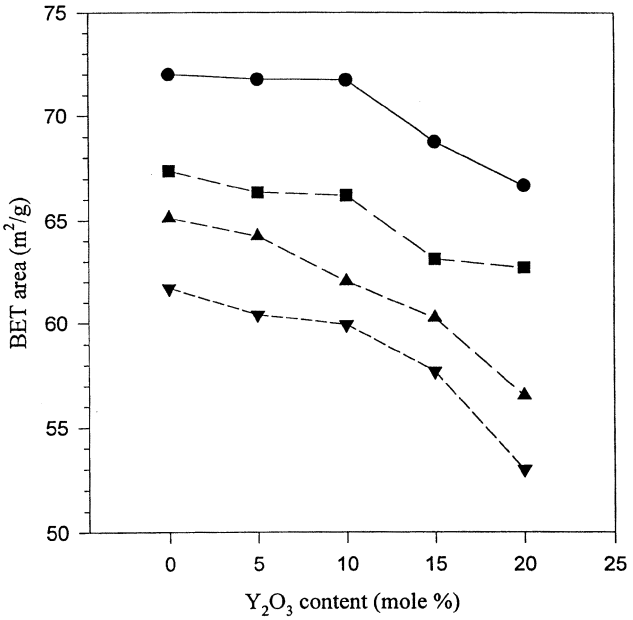

Figure 1. Variation of BET areas with Y_2O_3 content in CeO_2 of YDC-modified γ-Al_2O_3 supports and catalysts. (●) YxCe20 supports; (■) 5CuYxCe20 catalysts; (▲) YxCe50 supports; (▼) 5CuYxCe50 catalysts. BET areas: γ-Al_2O_3 support, 115.6 m^2/g; 5Cu/γ-Al_2O_3 catalyst, 101.98 m^2/g.

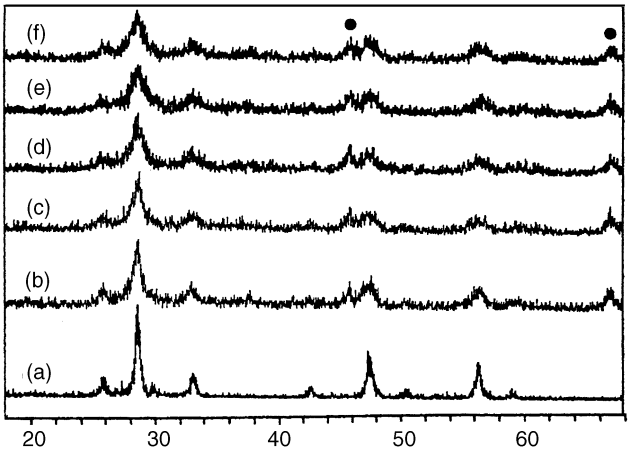

Figure 2. XRD patterns of (a) bulk Y5Ce100 prepared by co-precipitation, and 20 wt% YDC/γ-Al_2O_3 (YxCe20) supports (b) Ce20, (c) Y5Ce20, (d) Y10Ce20, (e) Y15Ce20, (f) Y20Ce20. The symbol ● designates peaks characteristic of γ-Al_2O_3. Operating conditions: Cu K_{α_1} radiation, 45 KeV, 40 mA; scan rate, 1°/min.

that the fluorite lattice structure of ceria had been preserved during the doping process. It is conceivable that, after calcination, a solid solution was formed between ceria and yttria and thus it is rational to infer that oxygen vacancies have been formed.

As is evident from figure 2, the diffraction profiles of YxCe20 supports, though broader in shape and smeared due to the background noise of γ-Al_2O_3, exhibit identical diffraction angles with those of the bulk Y5Ce100, except that the peaks of YxCe20 at 2θ *ca.* 46 and 67 which are absent in the pattern of bulk Y5Ce100 can be discriminated and assigned to γ-Al_2O_3. It is thus believed that, at 20 wt% loading on γ-Al_2O_3, YDC is dispersed within the structure of γ-Al_2O_3, so that the latter still exists plentifully on the surface of the supports.

The XRD patterns of YxCe50 supports depicted in figure 3 exhibit higher intensities than those of YxCe20

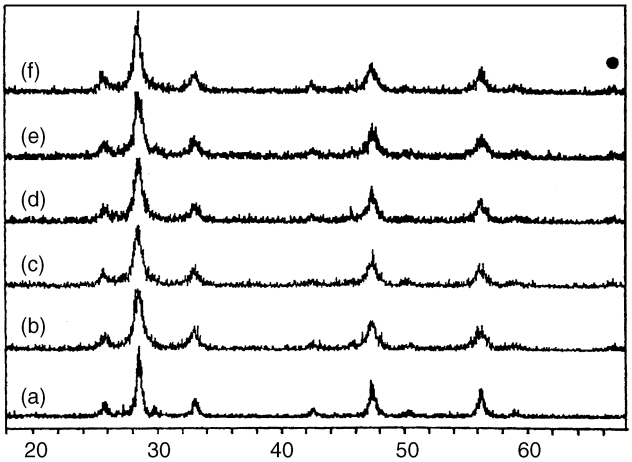

Figure 3. XRD patterns of (a) bulk Y5Ce100 prepared by co-precipitation, and 50 wt% YDC/γ-Al_2O_3 (YxCe50) supports (b) Ce50, (c) Y5Ce50, (d) Y10Ce50, (e) Y15Ce50, (f) Y20Ce50. The symbol ● designates peaks characteristic of γ-Al_2O_3. Operating conditions are the same as in figure 2.

of figure 2, and the peaks of γ-Al_2O_3 become increasingly undetectable. Thus, it can be reasonably presumed that for Y*x*Ce50 supports, ceria or YDC takes up most of the support surface area with less γ-Al_2O_3 being exposed. In addition, for Y*x*Ce50 supports the higher the yttria content is, the stronger the XRD signal intensity of the diffraction peak at $2\theta = 28.7^\circ$, characteristic of CeO2 (111) plane, becomes. Note that for supported crystalline oxides, the particle size of the oxide is proportional to its XRD signal intensity. It is suggested that the doping of yttria into the supported ceria leads to some crystal growth of ceria, thereby resulting in larger YDC particles and BET area loss. This result is in good agreement with those reported in the literature [28,30]. As a consequence, aggregation of ceria occurs more easily due to the yttria addition. A similar result was found by de Leitenburg *et al*. [31], who reported that the surface area decreased with the increase of dopant loading in zirconia-doped ceria solid solutions. However, as revealed in figure 2, the XRD signal intensification with the increase of yttria loading is not so obvious in the case of Y*x*Ce20 supports, probably because the signals were obscured by the relatively abundant γ-Al_2O_3 on the surface.

3.2. Temperature-programmed reduction

3.2.1. Hydrogen consumption

The amount of hydrogen consumption was determined by integration of the peak areas of TPR spectra of the catalysts. It has been well known that for ceria-supported precious metals, the amount of H_2 consumed in TPR is always higher than the amount required for the reduction of the metal precursor as reduction of surface Ce^{4+} occurs concurrently at low temperatures. As for Cu/YDC/γ-Al_2O_3 catalysts, it is worth addressing, for each catalyst, the ratio of the actual hydrogen consumption to that stoichiometrically required for copper reduction by evaluating the number of moles of hydrogen uptake divided by the number of moles of copper loading, giving the H_2/Cu ratios such as those listed in table 1. A distinct increase in the ratio is observed as ceria is loaded into γ-Al_2O_3, and this ratio increases with the increase of ceria addition, with the largest effect being observed for 5CuCe50. In addition, the ratio becomes less deviated from the theoretical value of unity with increasing yttria doping into ceria. These results indicate that partial reduction of ceria at low temperature is induced by and occurs concurrently with the reduction of supported copper oxide.

For precious metals, it has been observed that the metals supported on ceria can bring about a low-temperature reduction of surface-capping oxygen anions of ceria [20,32,33]. This phenomenon has been attributed to hydrogen spillover from the supported Group VIII metals to ceria [32–34]. The effect of hydrogen spillover does not seem to be working in the Cu–ceria system of the present study since hydrogen dissociation, the limiting step of spillover, would not occur easily to copper due to the difficulty of dissociative adsorption of hydrogen on copper at low temperatures [34–36]. A rational interpretation for the low-temperature partial reduction of ceria with supported copper is that with copper having been supported, the surface-capping oxygen anions of ceria are bonded to copper atoms to form the Cu–O–Ce bond linkages. The bond strength between the capping oxygen anion and cerium ion becomes weak due to formation of the linkage, thereby enabling partial reduction of ceria at low temperatures.

Table 1
Definition and compositions of catalysts, and the H_2/Cu ratios in temperature-programmed reduction.

Catalysts	CeO_2 or YDC loading in γ-Al_2O_3 (wt%)	Y_2O_3 content in YDC (mol%)	H_2/Cu
5CuAl	0	0	1.02
5CuCe20	20	0	1.17
5CuY5Ce20	20	5	1.16
5CuY10Ce20	20	10	1.14
5CuY15Ce20	20	15	1.11
5CuY20Ce20	20	20	1.08
5CuCe50	50	0	1.37
5CuY5Ce50	50	5	1.30
5CuY10Ce50	50	10	1.22
5CuY15Ce50	50	15	1.20
5CuY20Ce50	50	20	1.12

In practice, these shared oxygen anions are similar to the nested oxygen ions (NOIs) and, hence, can be reduced more readily than unshared surface-capping oxygen anions. When the NOI is reduced by H_2 and carried away as H_2O, an interfacial oxygen vacancy between the copper oxide species and ceria is formed. Gorte and co-workers [37–39] have concluded that the relative ease of oxygen removal in ceria may be due to the presence of defects, which are known to increase the rate of oxygen diffusion through ceria [40,41]. Thus, the reduction of NOI leads to a concentration gradient of oxygen vacancies in the surface layer of ceria. The gradient creates a driving force for lattice oxygen ions to diffuse progressively towards interfacial boundary *via* oxygen vacancies. This results in partial reduction of ceria at lower temperatures and marked increase in H_2/Cu ratios.

3.2.2. Effect of loading ceria into γ-Al_2O_3

As shown in figure 4, two peaks, namely β and γ, can be observed in the TPR profile of 5Cu/γ-Al_2O_3 catalyst. It is well recognized that when copper oxide is supported on γ-Al_2O_3, only two TPR peaks can be observed [29,42,43]. The formation of the β peak is attributed to the reduction of amorphous highly dispersed copper oxide species, while the γ peak is created due to the

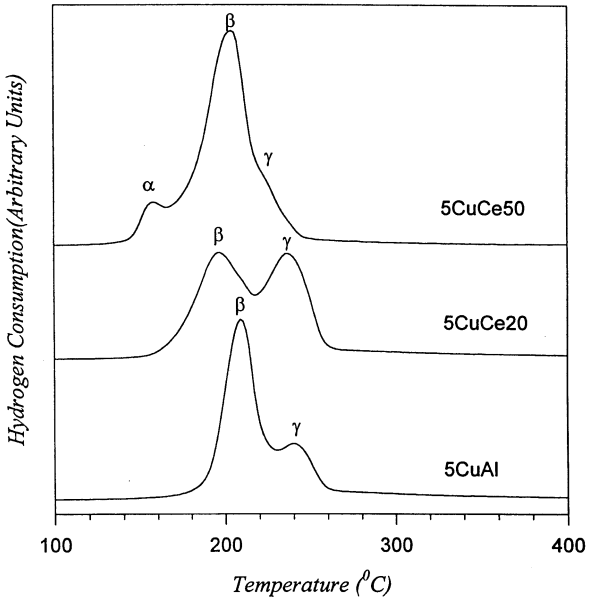

Figure 4. TPR patterns of 5CuAl, 5CuCe20, and 5CuCe50 catalysts. Operating conditions: 10 °C/min, 10% H_2 in N_2, with a total flow rate of 30 ml/min; sample weight, 200 mg.

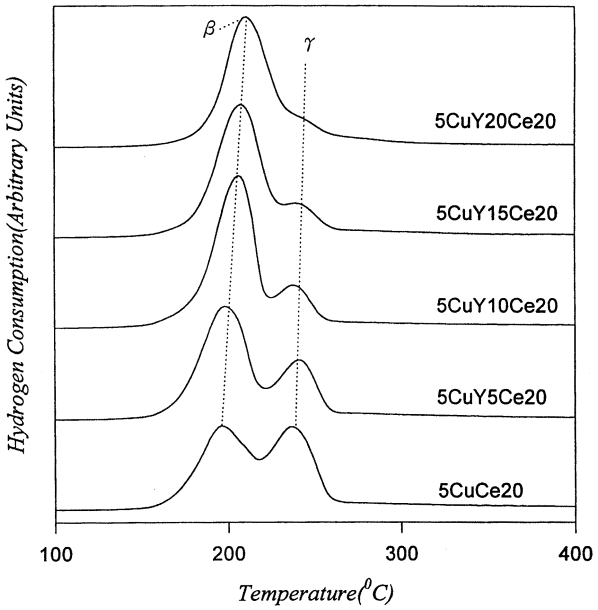

Figure 5. TPR patterns of 5CuYxCe20 catalysts. Operating conditions are the same as in figure 4.

reduction of crystalline bulk-like copper oxide phases [29,44]. It is clearly observable that the β- and γ-reduction peak temperatures shift downward after ceria has been loaded into the $\gamma\text{-}Al_2O_3$ support. This suggests that the dispersion of copper oxides is enhanced since it is known [29] that a higher dispersion of copper oxide leads to lower TPR reduction peak temperatures. Furthermore, with ceria loading increased to 50 wt%, the γ peak tends to shift further downward to become increasingly superimposed with the β peak. This result implies that at this ceria loading, the highly dispersed copper oxide becomes predominant.

At a ceria loading of 20 wt%, the α peak is not discernible in the TPR profiles of figures 4 and 5 due to the relatively low ceria loading on $\gamma\text{-}Al_2O_3$. When ceria loading is raised to 50 wt%, the α peak becomes distinguishable, as shown in the TPR patterns of figures 4 and 6. The formation of the α peak obviously resulted from the ceria addition. It is recognized [29] that the α-peak formation is attributed to the hydrogen consumption of interfacial oxygen ions of the copper oxide species having interaction with the surface oxygen vacancies of ceria, *i.e.*, the effect of interfacial metal oxide–support interaction (IMOSI). The amount of these copper oxide species is measured by the α-peak area. It is conceivable that, when ceria loading is raised to 50 wt%, the interaction occurring at the interface between copper oxides and surface oxygen vacancies of ceria becomes strong enough to enable the α-peak formation. This occurrence of the α peak relates well with the results of H_2/Cu ratios presented in table 1, which disclose that the catalysts with 50 wt% ceria loading exhibit higher values of H_2/Cu ratio than those with 20 wt% ceria content, and the H_2/Cu ratio of the 5CuCe50 catalyst is the most deviated from the theoretical value of one. It may thus be concluded that the H_2/Cu ratio becomes greater than one due to ceria addition and α-peak formation at low temperature owing to the presence of strong $Cu–Ce^{3+}$ interaction.

Recent investigations over mixed Cu–Ce oxides [45–47] reported that the strong interaction occurring at the interface between the highly dispersed copper oxide and ceria led to low-temperature reduction of copper oxide along with the partial reduction of ceria. These

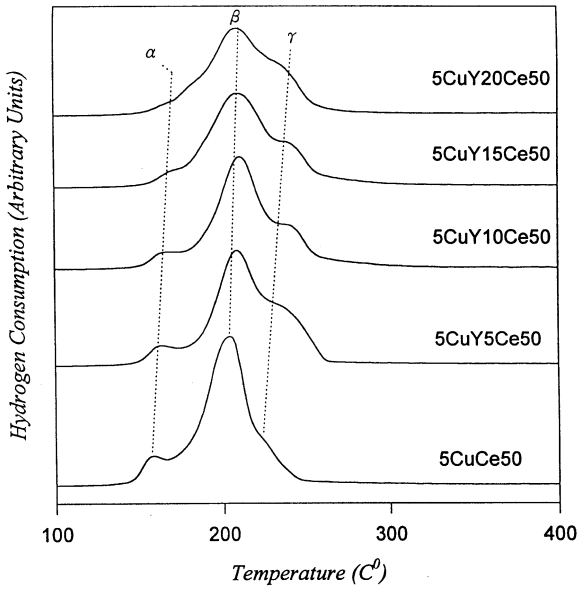

Figure 6. TPR patterns of 5CuYxCe50 catalysts. Operating conditions are the same as in figure 4.

findings agree well with our H_2/Cu results and TPR patterns of α-peak formation at low temperature.

3.2.3. Effect of yttria doping into ceria

The effect of yttria content, ranging from 5 to 20 mol% yttria in YDC, on the TPR behaviors of 5CuY*x*Ce20 and 5CuY*x*Ce50 catalysts are shown in figures 5 and 6, respectively. One can see from figure 6 that with increasing yttria loading into ceria, the α peak area, maximal at 5CuCe50, decreases and almost disappears with 20 mol% yttria content, while its peak temperature shifts to a higher value. The decline of the α peak area is clearly because of the decreasing surface oxygen vacancies of ceria having interaction with copper oxide species since, for fixed amount of 50 wt% loading of YDC onto alumina, the quantities of ceria and hence its surface oxygen vacancies become increasingly fewer as yttria content is increased. This corresponds well with the trend of the H_2/Cu ratio as shown in table 1, which falls progressively toward unity as the yttria content is increased.

It is of interest to observe from figures 5 and 6 that with increasing yttria content in ceria, the β- and γ-peak temperatures shift to higher values. This indicates that the reducibility of the copper oxide species can be lowered progressively by doping yttria into ceria. As pointed out earlier in this work, when yttria loading is increased the crystal growth of YDC leads to a loss in contact area between copper oxide and YDC. Thus, the particle-size increase of YDC and resulting loss in contact area with copper oxide is presumably believed to be responsible for the decrease of the reducibility of the β- and γ-peak copper oxide species and thus for their peak temperatures shifting toward higher ones. Because of the textural promoter effect of supported YDC on copper oxide, this loss of synergistically enhanced reduction of copper oxide by ceria agrees with studies in the literature that the reducibility of precious metals [48] or copper oxides [28] is lessened with increasing yttria content in ceria due to geometric reasons.

3.3. Steady-state activity of methanol synthesis

3.3.1. Effect of interfacial Cu–Ce^{3+} active centers

In this work, approaches have been employed to impart two different promotional effects to catalysts by loading ceria into γ-Al_2O_3 and doping yttria into ceria. These effects on the performances of catalysts for methanol synthesis from CO_2 and H_2 are compared in table 2. It is shown that the 5Cu/γ-Al_2O_3 catalyst is capable of producing methanol from CO_2 and H_2, but the activity and selectivity of methanol formation are comparatively low. The loading of ceria into 5Cu/γ-Al_2O_3 enhances substantially the selectivity and activity for CH_3OH formation, while CH_4 and CO formation is suppressed concomitantly. This indicates that following pre-reduction at 250 °C, the CeO_2 surface, aided by the formation of shared oxygen ion linkage Cu–O–Ce, has been partially reduced to non-stoichiometric CeO_{2-x}, and a synergy between copper oxide and the surface oxygen vacancies of ceria is at work. As a result, it is conceivable that the distinct enhancement of activity and selectivity toward methanol formation is due to the synergistic effect of copper oxide and the surface oxygen vacancies of ceria by means of formation of interfacial active centers, Cu–Ce^{3+}, as shown by earlier discussions on XRD and TPR of this work.

Table 2
Activity and selectivity of catalysts toward methanol formation. [a]

Catalysts [b]	CH_3OH Activity (μmol s^{-1} g^{-1})	Selectivity CH_3OH (%)	Selectivity CO (%)	Selectivity CH_4 (%)
5CuAl	0.90	54.91	44.54	0.55
5CuCe20	0.98	71.94	27.97	0.09
5CuY5Ce20	1.16	78.69	21.28	0.03
5CuY10Ce20	1.34	83.68	16.28	0.03
5CuY15Ce20	1.48	84.69	15.22	0.08
5CuY20Ce20	1.49	85.60	14.36	0.04
5CuCe50	1.14	75.98	21.90	2.12
5CuY5Ce50	1.46	85.70	13.03	1.27
5CuY10Ce50	1.91	86.29	12.43	1.28
5CuY15Ce50	1.86	86.69	12.77	0.54
5CuY20Ce50	1.83	90.60	9.03	0.38

[a] Reaction conditions: feed total gas flow rate = 100 ml/min with $H_2/CO_2 = 5$; catalyst weight = 1.0 g, pressure = 30 kg/cm^2, temperature = 250 °C.

[b] Pre-reduced by H_2 at a flow rate of 100 ml/min for 8 h at 250 °C under the pressure of 10 kg/cm^2.

Owing to the effect of the Cu–Ce^{3+}interfacial active centers, it is rational that the 5CuY*x*Ce50 catalysts, in spite of their lower BET areas, exhibit higher activity and selectivity toward methanol formation than the 5CuY*x*Ce20 catalysts. Therefore, it may be concluded that the catalytic activity is governed by the oxygen vacancies of ceria and interfacial active centers formed rather than by the dispersion or BET area provided by γ-Al_2O_3.

In fact, in CO_2 hydrogenation, the role of ceria in precious metal–CeO_2 catalysts in promoting activation of CO_2 at the interface between ceria and metal crystallites has been recognized to lie in the ability of ceria to create surface and bulk vacancies and in the effectiveness of the Ce^{3+}/Ce^{4+} redox couple [23,24]. Employing the Pd/CeO_2 catalyst to study the hydrogenation of CO_2 to methanol, Fan and Fujimoto [10,11] indicated that partial reduction of CeO_2 was facilitated, with the aid of hydrogen spillover from Pd, to enable the low-temperature formation of surface Ce^{3+}. In addition, Le Normand *et al.* [49] observed, in a study on syngas conversion over Pd supported on rare earth oxides, that a high selectivity to methanol correlated strongly

with the occurrence of interfacial oxygen vacancies of ceria at the Pd–ceria support interface.

3.3.2. Effect of intrinsic oxygen vacancies of YDC and yttria content

Several studies on ceria have pointed out the important role of surface Ce^{3+} species in the activation of molecules like CO or CO_2 with the aid of the participation of lattice oxygen [23,24,40]. It is clearly observable from table 2 that the activity and selectivity toward methanol formation is enhanced by doping yttria into ceria, and this promotional effect augments with increasing yttria content in ceria. It is known from defect chemistry that the rate of oxygen transport, as well as the total number of oxygen vacancies, can be enhanced by doping ceria with an aliovalent cation [25,50,51], which is yttria doping in this study. For YDC, anionic oxygen vacancies exist as structural defects due to the non-stoichiometric nature of the fluorite-type solid solution. The bulk Ce^{3+} oxygen vacancies in the ''as-synthesized'' YDC are created intrinsically as stable forms of non-stoichiometric oxides, thereby able to exist relatively plentifully in a stabilized manner under the milder reduction conditions of methanol synthesis. Consequently, the gradient of vacancy concentration from the bulk of YDC to the surface can steadily provide additional oxygen vacancies to the surface for activation of CO_2. In other words, the supply of bulk oxygen vacancies to the surface to activate CO_2 can be sustained in YDC during reaction.

For CeO_2-supported catalysts, Trovarelli and coworkers [23,24] also provided strong evidence of participation of bulk CeO_2 in the enhancement of the activation of CO_2 by surface oxygen vacancies of ceria. However, for their undoped ceria system, since the bulk oxygen vacancies created extrinsically by high-temperature reduction of ceria at 500 °C are limited in number and are unlikely to be regenerated under the milder reduction conditions during reaction, the annihilation of the bulk vacancies by the oxygen from CO_2 dissociation is permanent, so that their catalytic activity enhancement is only transient and thus cannot be sustained [23,24].

With increasing yttria doping into ceria, increasing numbers of bulk oxygen vacancies can participate steadily in the activation of CO_2, thereby leading to the observed enhanced steady-state catalytic activity and selectivity toward methanol formation. Accordingly, as presented in table 2, the higher the yttria content in ceria, the higher the methanol activity and selectivity that can be obtained, although there exists some slight discrepancy in the methanol activities, probably due to the already very high activities of the 5CuY*x*Ce50 catalysts when the yttria content is higher than 10 mol%. Note that for 5CuCe20 or 5CuCe50 catalysts following pre-reduction at 250 °C, bulk oxygen vacancies of ceria were not likely to be formed [10,11,23], so that less activity and selectivity for methanol formation is expected for these catalysts, as compared with those of the 5CuY*x*Ce20 or 5CuY*x*Ce50 catalysts.

4. Conclusions

The effects of surface oxygen vacancies of yttria-doped ceria (YDC) and the yttria content in ceria on the activity and selectivity of copper oxide catalysts for methanol synthesis have been studied. Based on the results of this work, the following conclusions can be made:

1. The activity and selectivity of copper oxide catalysts for methanol synthesis from CO_2 hydrogenation can be markedly enhanced by loading ceria into γ-Al_2O_3 and by doping yttria into ceria to form a non-stoichiometric YDC.
2. The activity and selectivity enhancement is inferred to result from the synergistic effect of copper oxide and the surface oxygen vacancies of ceria by means of the formation of interfacial active centers. Because of the effect of interfacial active centers, the higher the ceria loading level in γ-Al_2O_3, the higher the methanol activity and selectivity that can be achieved. The catalytic activity is governed by the oxygen vacancies of ceria and interfacial active centers formed rather than by the dispersion or BET surface area provided by γ-Al_2O_3.
3. Partial reduction of ceria at low temperature is induced by and occurs concurrently with the reduction of supported copper oxide. The bulk Ce^{3+} oxygen vacancies in yttria-doped ceria are created intrinsically as structural defects, and their supply to the surface to activate CO_2 is sustained under the reaction conditions of methanol synthesis.
4. With increasing yttria doping into ceria, increasing numbers of bulk oxygen vacancies can participate steadily in the activation of CO_2, thereby leading to the observed enhancement of the steady-state activity and selectivity toward methanol formation. In this regard, the enhancement can be designed by using an anion-deficient YDC support and by increasing the yttria content in ceria.
5. When copper oxide is supported on CeO/γ-Al_2O_3 composite supports, the resulting synergistic effect between copper oxide and the surface oxygen vacancies of ceria lowers the TPR peak temperature of the copper oxide species and forms the α-peak.
6. When yttria content is increased, the particle-size increase of YDC and resulting loss of its contact area with copper oxide is believed to be responsible for the poor reducibility of the β- and γ-peak copper oxide species and thus for their TPR peak temperatures shifting toward higher values.

References

[1] E. Ramarson, R. Kieffer and A. Kinnemann, Appl. Catal. 4 (1982) 281.
[2] B. Denise and R.P.A. Sneeden, Appl. Catal. 28 (1986) 235.
[3] Y. Amenomiya, Appl. Catal. 30 (1987) 57.
[4] G.C. Chinchen, K.C. Waugh and D.A. Whan, Appl. Catal. 25 (1986) 101.
[5] G.C. Chinchen, M.S. Spencer, K.C. Waugh and D.A. Whan, J. Chem. Soc. Faraday Trans. 83 (1987) 2193.
[6] R. Burch, S.E. Golunski and M.S. Spencer, J. Chem. Soc. Faraday Trans. 86 (1990) 2683.
[7] G.J.J. Bartley and R. Burch, Appl. Catal. 43 (1988) 141.
[8] B. Denise, O. Cherifi, M.M. Bettahar and R.P.A. Sneeden, Appl. Catal. 48 (1989) 365.
[9] J.C. Frost, Nature 334 (1988) 577.
[10] L. Fan and K. Fujimoto, Appl. Catal. A 106 (1993) L1.
[11] L. Fan and K. Fujimoto, J. Catal. 150 (1994) 217.
[12] S.J. Tauster, S.C. Fung and R.L. Garten, J. Amer. Chem. Soc. 100 (1978) 170.
[13] G.L. Haller and D.E. Resasco, Adv. Catal. 36 (173) 1989.
[14] R. Burch and A.R. Flambard, J. Catal. 78 (1982) 389.
[15] I.S. Metcalfe and S. Sundaresan, AIChE J. 34 (1988) 195.
[16] C.B. Choudhary, H.S. Maiti and E.C. Subbarao, in: *Solid Electrolytes and Their Applications*, ed. E.C. Subbarao (Plenum Press, New York, 1980) p. 47.
[17] R. Gerhardt-Anderson and A.S. Nowick, Solid State Ionics 5 (1981) 547.
[18] J.L.G. Fierro, J. Soria, J. Sanz and J.M. Rojo, J. Solid State Chem. 66 (1987) 154.
[19] E. Abi-Aad, R. Bechara, J. Grimblot and A. Aboukais, Chem. Mater. 5 (1993) 793.
[20] H.C. Yao and Y.F. Yu Yao, J. Catal. 86 (1984) 254.
[21] J.C. Summers and S.A. Ausen, J. Catal. 58 (1979) 131.
[22] C. Sudhakar and M.A. Vannice, Appl. Catal. A 14 (1985) 47
[23] A. Trovarelli, C de Leitenburg, G. Dolcetti and J. Llorca, J. Catal. 151 (1995) 111.
[24] C de Leitenburg, A. Trovarelli and J. Kaspar, J. Catal. 166 (1997) 98.
[25] B.K. Cho, J. Catal. 131 (1991) 74.
[26] T.H. Etsell and S.N. Flengas, Chem. Rev. 70 (1970) 339.
[27] J.B. Wang, W.-H. Shih and T.J. Huang, Appl. Catal. A 203 (2000) 191.
[28] W.P. Dow, Y.P. Wang and T.J. Huang, Appl. Catal. A 190 (2000) 25.
[29] W.P. Dow and T.J. Huang, J. Catal. 160 (1996) 155.
[30] R.K. Usmen, G.W. Graham, W.L.H. Watkins and R.W. McCabe, Catal. Lett. 30 (1995) 53.
[31] C. de Leitenburg, A. Trovarelli, F. Zamar, S. Maschio, G. Dolcetti and J. Llorca, J. Chem. Soc. Chem. Commun. (1995) 2181.
[32] A. Trovarelli, G. Dolcetti, C de Leitenburg, J. Kaspar, P. Finetti and A. Santoni, J. Chem. Soc. Faraday Trans. 88 (1992) 1311.
[33] T. Yamada, K. Kayano and M. Funabiki, in: *New Aspects of Spillover Effect in Catalysis*, eds. T. Inui, K. Fujimoto, T. Uchijima and M. Masai (Elsevier, Amsterdam, 1993) p. 329.
[34] J. El Fallah, S. Boujana, H. Dexpert, A. Kiennemann, J. Majerus, O. Touret, F. Villain and F. Le Normand, J. Phys. Chem. 98 (1994) 5522.
[35] C.N. Satterfield, *Heterogeneous Catalysis in Industrial Practice*, 2nd edition (McGraw-Hill, New York, 1991) p. 175.
[36] S.J. Teichner, Appl. Catal. 62 (1990) 1.
[37] E.S. Putna, J.M. Vohs and R.J. Gorte, J. Phys. Chem. 100 (1996) 17862.
[38] H. Cordato, T. Bunluesin, J. Stubenrauch, J.M. Vohs and R.J. Gorte, J. Phys. Chem. 100 (1996) 785.
[39] G.S. Zafiris and R.J. Gorte, J. Catal. 139 (1993) 561.
[40] T. Jin, T. Okuhara, G.J. Mains and J.M. White, J. Phys. Chem. 91 (1987) 3310.
[41] M.G. Sanchez and J.L. Gazquez, J. Catal. 104 (1987) 120.
[42] R. Deen, P.I.T. Scheltus and G. de Vries, J. Catal. 41 (1976) 218.
[43] R.M. Friedman, J.J. Freeman and F.W. Lytle, J. Catal. 55 (1978) 10.
[44] M. Shimokawabe, H. Asakawa and N. Takezawa, Appl. Catal. 59 (1990) 45.
[45] W. Liu and M. Flytzani-Stephanopoulos, J. Catal. 153 (1995) 304.
[46] E. Abi-Aad, A. Bennani, J.P. Bonnelle and A. Aboukais, J. Chem. Soc. Faraday Trans. 91 (1995) 99.
[47] G. Wrobel, C. Lamenter, A. Bennani, A. D'Huysser and A. Aboukais, J. Chem. Soc. Faraday Trans. 92 (1996) 2001.
[48] J.G. Nunan, M.J. Cohn and J.T. Donner, Catal. Today 14 (1992) 277.
[49] F. Le Normand, J. Barrault, R. Breault, L. Hilaire and A. Kiennemann, J. Phys. Chem. 95 (1991) 257.
[50] H.L. Tuller and A.S. Nowick, J. Electrochem. Soc. 122 (1975) 255.
[51] H.L. Tuller and A.S. Nowick, J. Electrochem. Soc. 126 (1979) 209.